Acta Cryst. (1977). B33, 335–343

The Structure of Sickling Deer Type III Hemoglobin by Molecular Replacement

BY W. C. SCHMIDT JR, R. L. GIRLING, T. E. HOUSTON, G. D. SPROUL AND E. L. AMMA

Department of Chemistry, University of South Carolina, Columbia, South Carolina 29208, *USA*

AND T. H. J. HUISMAN

Department of Cell and Molecular Biology, Medical College of Georgia, Augusta, Georgia 30392, *USA*

(*Received* 26 *April* 1976; *accepted* 15 *June* 1976)

A combination of oriented single-crystal electron microscopy and protein crystallography has been used to show that crystalline sickling deer hemoglobin molecules from *Odocoileus virginianus* [oxy β-chain variant-type III, Hb(DIII)] pack to form a distorted honeycomb (hexagonal) structure with open solvent channels. This network of molecules, consisting of out-of-register anti-parallel strands (fibrils), bears an unmistakable relation to the hemoglobin fibers and aggregates found in human sickled cells. The crystal structure was solved by means of the rotation and translation functions, with data to 3·5 Å resolution giving the current residual of 0·430. Oxy- or cyanomet-Hb(DIII) crystallizes in space group $C2$ with $a = 163{\cdot}49\,(3)$, $b = 70{\cdot}83\,(2)$, $c = 65{\cdot}95\,(2)$ Å, $\beta = 94{\cdot}15\,(1)°$ and $Z = 4$.

Introduction

Of the many human hemoglobin variants known, none has received greater attention than sickle cell hemoglobin (HbA → HbS; 6βA3 glu → val). Its clinical manifestations are well known (Huisman, 1972; Milner, 1974; Barnhart, Henry & Lusher, 1974) and considerable interest exists (Wishner, 1974; Bertles, 1974; White, 1974) concerning the structure of this molecule and the nature of its intermolecular contacts in sickling. The Virginia white-tailed deer, *Odocoileus virginianus*, with hemoglobin β-chain variant known as type III [hereafter Hb(DIII)] also develops sickled erythrocytes (Simpson & Taylor, 1974; Taylor & Easley, 1974; Kitchen, Putnam & Taylor, 1964, 1967), albeit in the oxy form. Fiber formation as well as many of the other molecular properties of HbS (Girling, Houston, Sproul, Schmidt, Plese & Amma, 1976; Amma, Sproul, Wong & Huisman, 1974; Finch, Perutz, Bertles & Döbler, 1973) can be directly related to sickled Hb(DIII). In view of the high correlation between HbS and Hb(DIII), it seems likely that a detailed protein crystal structure analysis of Hb(DIII) would add much significant information to the sickling phenomenon. We report here the crystal growth, oriented single-crystal electron microscopy, X-ray data collection techniques, structure solution by the rotation–translation functions, and some details of the molecular packing. A more detailed analysis of the structure and its biological significance will be published at a later date.

Experimental

Samples of blood from deer number 530 that is homozygous for deer hemoglobin β type III were obtained from the School of Veterinary Medicine, University of Georgia, Athens, GA. Hemolysates were prepared by standard procedures (Harris, Wilson & Huisman, 1972).

Diffraction-quality crystals of either oxy- or cyanomet-Hb(DIII) were grown by dialysis of a buffered (1·6 *M* phosphate, *p*H 6·3) 3·0 g% Hb(DIII) solution against $(NH_4)_2SO_4$ solutions with a modified Zeppezauer (1971) micro dialysis cell. The $(NH_4)_2SO_4$ solutions, graded between 0·25 and 0·45 *M*, were buffered with monobasic sodium and dibasic potassium phosphates at concentrations of 2·85 *M* and 2·90 *M* phosphate at *p*H 6·3. In addition, the cyanomet-Hb(DIII) buffer solutions contained a trace of sodium cyanide. Crystals grew as trapezoidal plates over a period of several weeks. The crystals are elongated along the [001] direction and are bound on the ends and sides by the (111) and (010) planes, respectively, and on the plate faces by the (100) planes. Diffraction-quality crystals could be grown as large as 5 × 2 × 1 mm.

For diffraction studies, these crystals were oriented in thin-walled glass capillaries so that the [001] direction of the crystal corresponded to the capillary axis. The capillaries containing the crystal and a small amount of mother liquor were sealed with low-melting dental wax and optically aligned on goniometer heads using the well defined crystal morphology.

Precession photographs on a Huber 100 mm camera were taken of the *nkl* ($n = 0, 1, 2, 3, 4, 5$) and *hnl* ($n = 0, 1, 2$) zones. Systematic extinctions (for *hkl*, $h + k = 2n + 1$) show that the crystals must belong to one of the space groups $C2$, $C2/m$, or Cm. The chirality of Hb(DIII) specifies $C2$ uniquely. Unit-cell constants, $a = 163{\cdot}49$ (3), $b = 70{\cdot}83$ (2), $c = 65{\cdot}95$ (2) Å, $\beta = 94{\cdot}15$ (1)°, were determined by a least-squares fit to the setting angles of 18 reflections which were hand-centered on a Picker FACS-1 diffractometer equipped with a graphite monochromator and a standard focus Cu tube. Space-filling considerations and a calculated protein density of 1·2 (1) g cm^{-3} obtained from flotation measurements in both aqueous Cs_2SO_4 and chlorobenzene/bromobenzene/ethylene bromide solutions showed $Z = 4$.

Electron microscopy

Single crystals for electron microscopic examination were fixed by first soaking in 1–2 ml mother liquor containing 2% gluteraldehyde for 2 h. The gluteraldehyde solution was then decanted, mother liquor containing 1% osmium tetroxide was added, and the crystals were soaked for 1 h. Following this soak, the fixative solution was decanted, and the crystals were rinsed with mother liquor. The ionic buffer residue was removed and the crystals dehydrated by washing with successively increasing concentrations of ethanol in water, starting with 40% ethanol and terminating with absolute ethanol. To avoid sudden changes in the solvent of crystallization and to prevent buffer precipitation on the crystals, the cloud point was reached at each stage

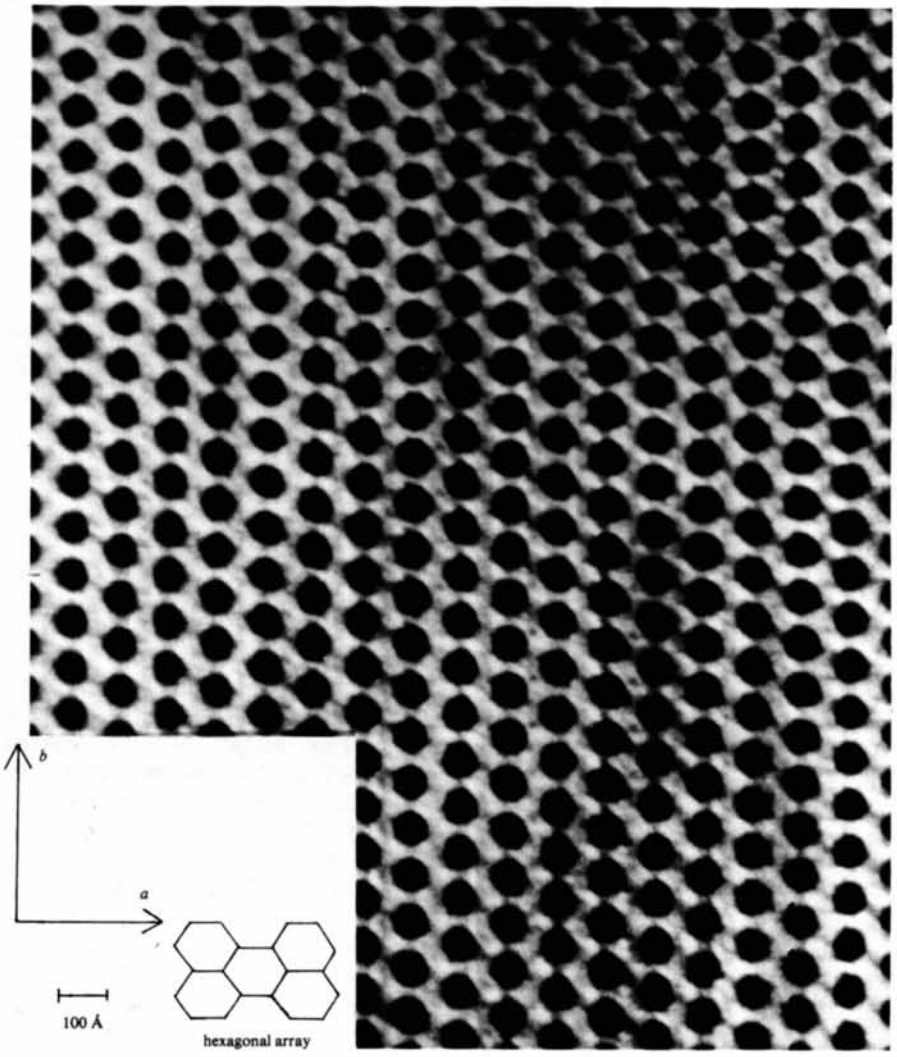

Fig. 1. Electron micrograph (90 000×) of oxy- or cyanomet-Hb(DIII) crystals which have been fixed, sectioned and strained as indicated in the text. The [100] direction is horizontal. This section is approximately normal to [001] and shows the optically averaged (Markham, Frey & Hills, 1963; Markham, Hitchborn, Hills & Frey, 1964) honeycomb or hexagonal array where the dark areas correspond to holes in the lattice. The model hexagonal array is given in the lower left-hand corner.

and then back titrated with a more dilute solution. After dehydration, the crystals were embedded in standard Spurr medium following published procedures (Spurr, 1969).

Crystals with readily identifiable crystal faces were chosen for sectioning. These were cut from the polymerized Spurr block and visually aligned on a microtome such that the [001] or [010] direction was perpendicular to the diamond knife. A Dupont knife with an included angle of 58° was used to cut sections of approximately 0·10 mm thickness which were mounted on 200 mesh uncoated copper grids. These mounted samples were stained for 1 h with 5% uranyl acetate (Watson, 1958) and rinsed with distilled water.

Transmission electron micrographs (Figs. 1 and 2) of the sections were made on a JEOL JEM 100B electron microscope operated at 80 kV, with an anti-contamination device, a 20 μm objective aperature and a high-resolution specimen holder. Negatives were calibrated using a grating replica (2160 lines mm^{-1}, E. Fullam, Inc.).

Intensity data collection

Diffraction intensity data were collected on a modified Picker FACS-1 diffractometer. The crystal to counter

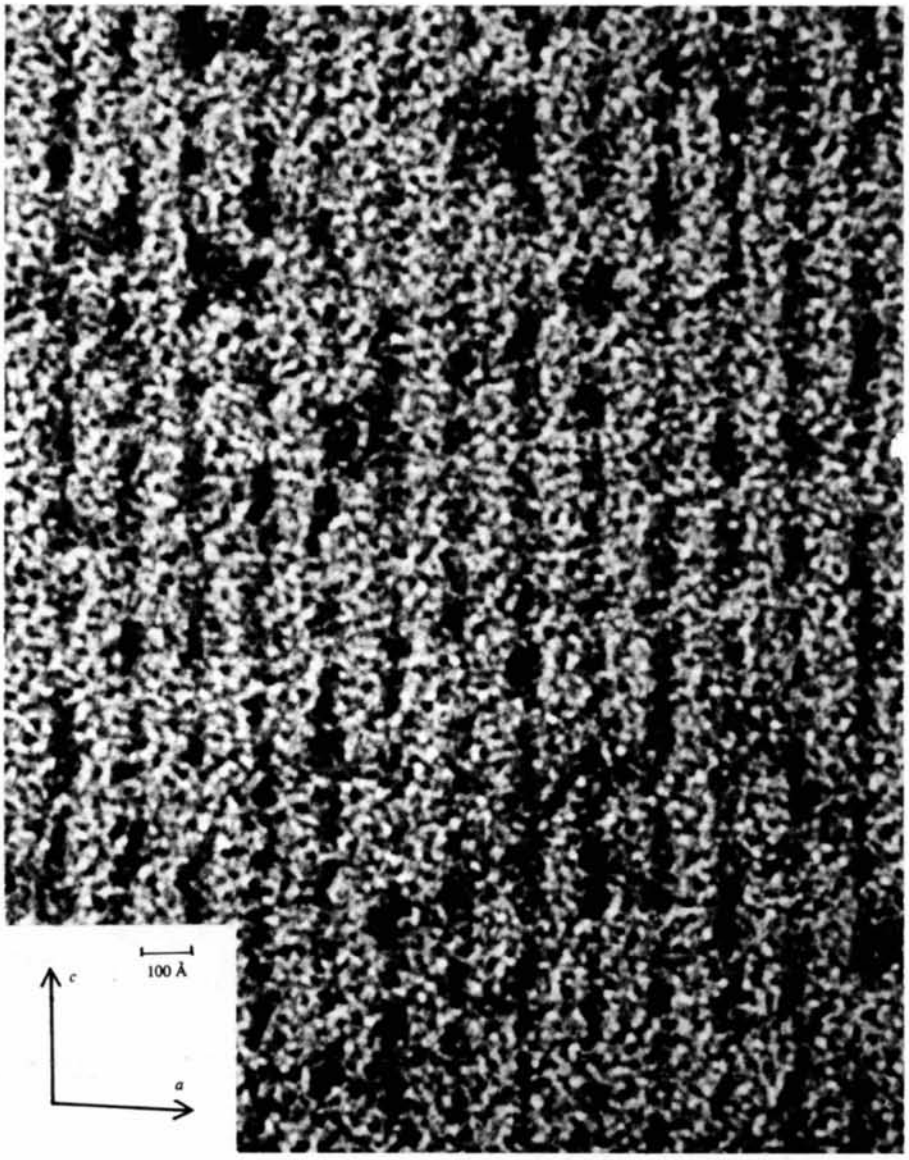

Fig. 2. Electron micrograph (90 000×) of oxy- or cyanomet-Hb(DIII) crystals which have been fixed, sectioned and stained as indicated in the text. The [100] direction is horizontal. This section is normal to [010] and reveals the ribbon-like extents of fibrils or filaments parallel to the [001] direction.

distance was increased to 71·0 cm with an extended 2θ arm, and a He-gas-filled beam tunnel was inserted between the diffracted beam collimator and counter. The gas was also circulated through the monochromator housing. The monochromator angle was set at $2\theta_m = 26{\cdot}34°$ for Cu radiation with a large take-off angle of 4·5°. All crystals were aligned in the same relative orientation in order to minimize intercrystal differences. The FACS-1 data collection software was revised to provide intensity measurements in the following way (Girling, Abola & Wood, 1977): individual intensities were measured by a series of four ω stepscans of 10 s duration ($\Delta\omega = 0{\cdot}04°$ between successive steps) near the peak maximum followed by background samples at either side of the peak. If the relatively flat peak maximum was not completely contained within this range, an additional measurement was made on the deviant end. The *hkl* values and these six or seven intensity measurements were then punched on paper tape, transferred to magnetic tape and processed by the IBM 370/168. The integrated intensity was estimated by subtracting the time-scaled background from the sum of the three highest adjacent ω peak counts. Only those reflections whose peak intensity exceeded 3σ were stored for further use. The total peak count, N_T, used in the calculation of σ (Stout & Jensen, 1968) is the sum of the three highest adjacent ω peak counts.

Initially a set of 5·5 Å data were collected by the more standard moving ω scan technique. These data were in excellent agreement with the ω stepscan data above, but had inferior intensity statistics. The ω stepscan was therefore judged the superior method, especially for the weaker reflections. Absorption correction, scaling and decay sets (see below) were collected in essentially the same ω stepscan mode except that the *hkl*'s and setting angles were stored on the IBM 370/168 disk file and accessed *via* APL-SV (IBM interactive language), telephone lines and a Bell 1800 modem (Gash, Reeves & Amma, 1976).

Determination of decay characteristics

In order to define the decomposition characteristics of this particular crystalline protein, a crystal was exposed to X-rays in the data collection mode until the intensities had decreased from their initial values by 30%. Such data sets were collected for six 2θ ranges (Fig. 3), and the data in these ranges were further divided into three groups on the basis of intensity. The decay factor in each data set remained reasonably linear until the intensities had decreased from their initial values by 15%. Beyond this point, the decay was unpredictable. Decay dependence upon 2θ was obvious, but the dependence upon intensity was not clear-cut and therefore the intensity decay variation was averaged for a given 2θ range.

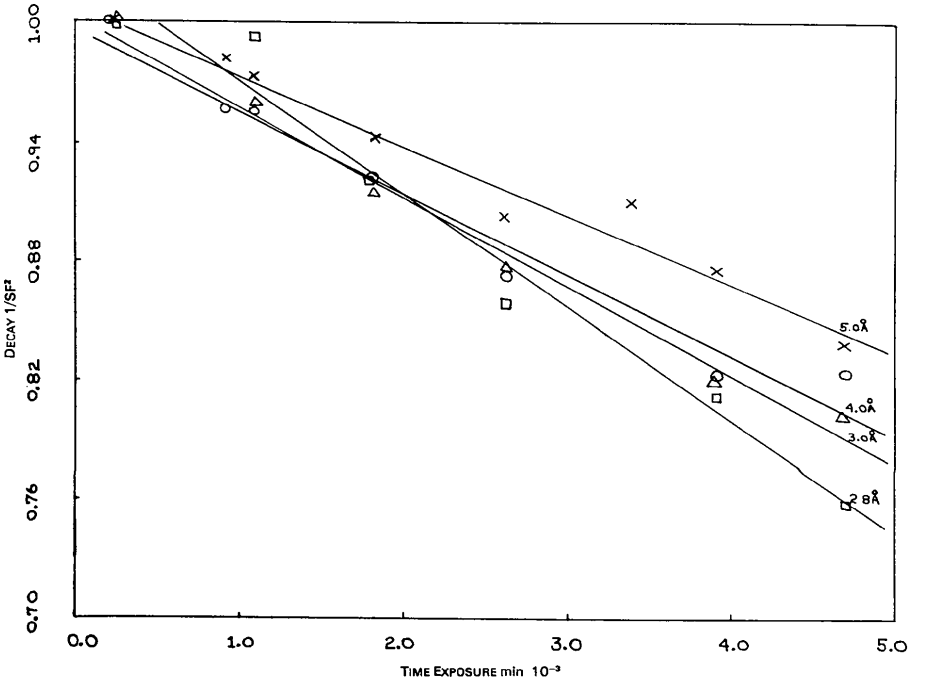

Fig. 3. The points □, △, □, × represent the normalized net intensity *vs* exposure time (decay) of a set of ~ 150 reflections in the resolution ranges of 2·8–3·0, 3·0–4·0, 4·0–5·5 and 5·0–∞ Å respectively for a single crystal of Hb(DIII). Each line is a least-squares fit to the points within one of these ranges and it is clear that the decay rates increase with higher-order data. The reflections, chosen randomly to represent 2θ, χ, φ and intensity values for a given range, were collected by ω scans (1° min^{-1}) with two 10 s background measurements.

From these results it was decided that data collection for a given crystal should be terminated when the average intensity of a decay set decreased from the average initial intensity by 15%, and that the decay correction must be applied as a function of 2θ (multiple sets). In addition, three standard reflections were measured after every 50 intensity measurements to monitor both crystal decay and alignment; these were the 31,7,6, 1,17,6 and the $\bar{1}8$,12,5 Bragg reflections.

Absorption corrections

The empirical absorption correction of North, Phillips & Mathews (1968) was applied to the data from each crystal. The 0,0,18 reflection at $2\theta \sim 24°$ was measured in 5° intervals for a full 360° φ rotation prior to the initiation and termination of data collection. This reflection was chosen because it was in the *mid*-2θ-range of the data and was sufficiently intense for good counting statistics.

Scaling of data

The data from individual crystals were scaled together *via* the lowest-resolution decay set gathered prior to data collection. The intensity differences between scaled, identical data from different crystals were routinely $\gtrsim 5\%$.

Structure solution

The molecular replacement technique pioneered by Rossmann (1972) relies on the similarity of at least the secondary and tertiary structures of macromolecules to solve an unknown crystal structure. The 'unknown' structure is solved at low resolution by rotating and translating a model until it is correctly located in the unit cell (Tollin, 1969; Lattman, Nockolds, Kretsinger & Love, 1971; Joynson, North, Sarma, Dickerson & Steinrauf, 1970; Fehlhammer, Schiffer, Epp, Colman, Lattman, Schwager, Steigemann & Schramm, 1975). Hemoglobin structures are particularly well adapted for the application of this technique (Prothero & Rossmann, 1964; Lattman & Love, 1970; Ward, Wishner, Lattman & Love, 1975) since the secondary, tertiary and, to a lesser degree, quaternary structures of these molecules are relatively invariant.

We have used the horse oxyhemoglobin molecule as the model to determine the phases at low resolution of Virginia white-tailed deer (*Odocoileus virginianus*) Hb(DIII) (Schmidt, Girling, Sproul & Amma, 1976) X-ray data.

The rotational and translational search procedures described by Lattman & Love (1970) and Crowther & Blow (1967), respectively, were used to overcome the phase problem. The 5 Å molecular diffraction pattern (structure factors) for the model molecule, $F_M(\mathbf{h})$, used in both search procedures was calculated using the expression:

$$\sum_n f_n \sum_m \exp 2\pi i[\mathbf{h}(\boldsymbol{\rho}\mathbf{X}_{m,n})/s] = F_M(\mathbf{h})$$

where $\mathbf{h}$ is a reciprocal lattice vector, m is the number of atoms of a given type, n is the atom type, f_n is the scattering factor for the nth atom type and $\mathbf{X}_{m,n}$ is the set of Cartesian horse oxyhemoglobin coordinates (Perutz, Muirhead, Cox & Goaman, 1968; *via* Koetzle, 1974) used in the calculation. The Cartesian **a**, **b** and **c** directions correspond to **a**, **b** and **c*** in the horse hemoglobin unit cell. $\boldsymbol{\rho}$ is the Eulerian rotation matrix of Rossmann & Blow (1962) whose elements in this application are

0·242	0·000	−0·970
0·000	1·000	0·000
0·970	0·000	0·242.

The operation $(\boldsymbol{\rho}\mathbf{X}_{m,n})/s$ (where $s = |\mathbf{a}| = |\mathbf{b}| = |\mathbf{c}|$) gives fractional coordinates from horse atomic coordinates which have been rotated by −76° about the molecular twofold axis to conform with preliminary packing considerations ($\theta_1 = 270°$, $\theta_2 = -76°$, $\theta_3 = 90°$), and placed in an orthogonal cell ($a = b = c = 200$ Å) of $P1$ symmetry such that the molecular twofold and crystallographic b axes are coincident. The symmetry of space group $P2$ is generated by virtue of this coincidence.

The calculation performed by the rotation function is given by the expression

$$R(\boldsymbol{\rho}) = \sum_{\mathbf{h}} F_2^2(\boldsymbol{\rho}^T\mathbf{h}) F_M^2(\mathbf{h})$$

where $\boldsymbol{\rho}^T$ is the transpose of the rotation matrix, $\boldsymbol{\rho}$, $F_2^2(\mathbf{h})$ is the square of an observed Hb(DIII) structure amplitude and $F_M^2(\mathbf{h})$ is the square of the molecular diffraction pattern at a given reciprocal lattice point $\mathbf{h}$. The calculation corresponds to a superposition of two Patterson functions where large values of $R(\boldsymbol{\rho})$ indicate a high degree of coincidence between the unknown and model molecule. Lattman (1972) has used modified Eulerian angles, θ_+, θ_2, θ_-, where $\theta_+ = \theta_1 + \theta_3$, $\theta_- = \theta_1 - \theta_3$ in order to produce a more efficient sampling of $R(\boldsymbol{\rho})$. Based on this sampling procedure, the rotation function was calculated in the angular range $0° \le \theta_+ \le 270°$, $0° \le \theta_2 \le 180°$ and $-90° \le \theta_- \le 180°$ in intervals of 10° and reflections with d spacings $\ge 5{\cdot}5$ Å and ≤ 20 Å were used. The map, a section of which is shown in Fig. 4, was scaled from 0–100 with the lowest contour level at 60 and succeeding contours in increments of 10. The r.m.s. deviation from the mean value of the map, 28, is 9·4. The two largest peaks, 7σ and 5σ above background respectively, are definitely significant. The highest peak (100) corresponds to the correct solution and the next highest (83) arises from the molecular pseudo-symmetry. The angular values for the solution were

refined by recalculating the rotation function near the peak region using 1° intervals, which improved θ_1, θ_2, and θ_3 (197°, 35°, 45°) by 3°, 2° and 5°, respectively, to give a matrix $\boldsymbol{\rho}$ with elements:

−0·507	−0·761	0·406
0·846	−0·347	0·406
−0·168	0·549	0·819.

The space group $C2$ of Hb(DIII) requires that the properly oriented molecule be placed correctly with respect to a symmetry element. The translation procedure of Crowther & Blow (1967) as coded by Lattman (Schmid, Herriott & Lattman, 1974) effectively searches all positions in the unit cell by means of the algorithm

$$T(\mathbf{t}) = \sum_{\mathbf{h}} \left\{ [\,|F_2(\mathbf{h})|^2 - \sum_{i=0}^{n-1} |F_M(\boldsymbol{\rho}\mathbf{S}_i\mathbf{h})|^2] \times F_M(\boldsymbol{\rho}\mathbf{S}_0\mathbf{h})\, F_M^*(\boldsymbol{\rho}\mathbf{S}_1\mathbf{h}) \exp(-2\pi i \mathbf{h}\mathbf{t}) \right\}.$$

A large value of $T(\mathbf{t})$, where $\mathbf{t}$ represents the required molecular shift, corresponds to coincidence of intermolecular Patterson vectors and is indicative of a solution. $\mathbf{S}_i$ is the ith symmetry operation in the space group of Hb(DIII). $\mathbf{S}_0$ is the identity operator and $\mathbf{S}_1$ ($s_{11} = s_{33} = -1$; $s_{22} = 1$; $s_{ij} = 0$, $i \neq j$) is the twofold symmetry operator of the symmetry element which must be positioned correctly with respect to the molecule. All other notation in the expression for $T(\mathbf{t})$ is identical to that used in the rotation function.

The map of the translation function, $T(\mathbf{t})$, calculated in the Harker section for this space group ($2x$, 0, $2z$) in the region $0 \leq x \leq 0{\cdot}5$ and $-0{\cdot}5 \leq z \leq 0{\cdot}5$ is shown in Fig. 5. The map was scaled from 0–100 with the lowest contour level at 30 and succeeding contours in increments of 10. The single peak which dominates the map at $t_u = 0{\cdot}316$, $t_w = 0{\cdot}414$, indicates that a displacement of the horse oxyhemoglobin molecule by $t_x = 0{\cdot}158$, and $t_z = 0{\cdot}207$ will properly position it in the Hb(DIII) unit cell.

The rotation and translation function solution places the atomic coordinates of the horse oxyhemoglobin molecule ($\mathbf{X}_{m,n}$) in the Hb(DIII) unit cell ($\mathbf{x}_{m,n}$) by the transformation:

$$\mathbf{O}\boldsymbol{\rho}\mathbf{X}_{m,n} + \mathbf{d} = \mathbf{x}_{m,n}$$

where $\mathbf{d}$ is the displacement $(t_x, 0, t_z)$ of the rotated ($\boldsymbol{\rho}$) and deorthogonalized ($\mathbf{O}$) (Rossmann & Blow, 1962) horse hemoglobin coordinates relative to the twofold symmetry element in the Hb(DIII) cell. The elements of $\mathbf{O}$ ($\times 10^3$) are:

6·14	0	0
0	14·1	0
1·11	0	15·2.

A structure factor calculation (Stewart, Kruger, Ammon, Dickinson & Hall, 1972) based on these atomic positions, using an isotropic thermal parameter of 30 Å^2 and 2232 reflections with d spacings between 5·5 and 11·0 Å, gave a conventional residual, R, of 43·9% where the scale factor, K, was determined by $K = \Sigma F_c(\mathbf{h})/\Sigma F_o(\mathbf{h})$.

The parameters θ_1, θ_2, θ_3, t_x and t_z were then refined (Table 1) by making small increments to the current value of each parameter separately and recalculating the residual using the updated atomic coordinates. The refined value for the parameter was taken as the one giving the minimum residual. Increments made to the Eulerian angles during refinement were 0·5°, extending to ±2·0° of the current value of the angles, and those made to the translational parameters were 0·25 Å, extending to ±1·0 Å of the current value of the parameters. Differences between the minimum and maximum

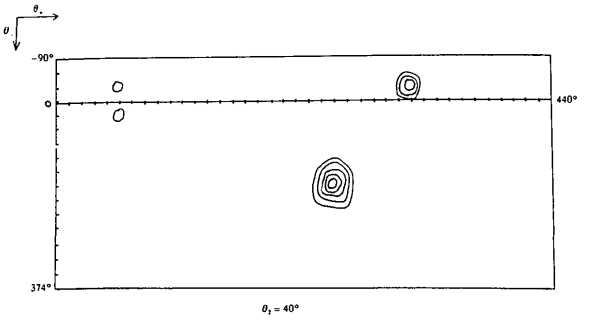

Fig. 4. A contoured section of the rotation function, $R(\boldsymbol{\rho})$ (calculated in 10° increments), containing the two largest peaks in θ_+, θ_2, θ_- space (see text for definition). The map is scaled from 0–100 with the lowest contour level at 60 and following contours incremented by 10. The r.m.s. deviation from the mean value of $R(\boldsymbol{\rho})$, 28, is 9·4. The two highest peaks, 7σ and 5σ above background respectively, can be interpreted as the correct solution (197°, 35°, 45°) and the correlation due to the pseudo-symmetry of the hemoglobin molecule.

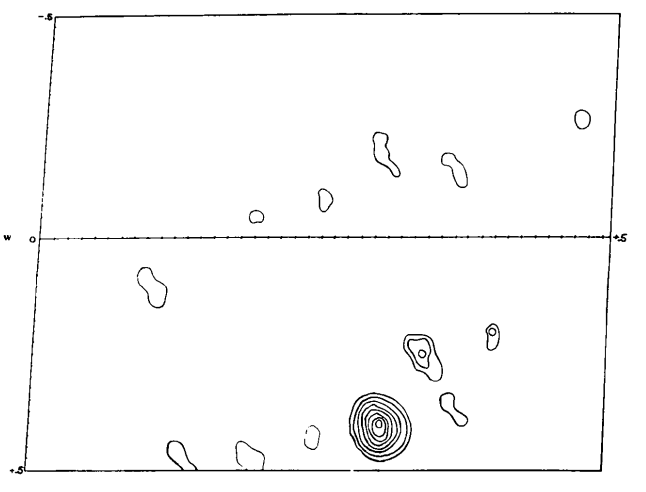

Fig. 5. A map of the u,0,w section of the translation function $T(\mathbf{t})$ in which points were calculated at 0·012 intervals in u and 0·025 in w. The scale and contour lines are as in Fig. 4 but the lowest contour is at 30. The solution is at $u = 0{\cdot}316$, $w = 0{\cdot}414$.

residuals during refinement of a single parameter were routinely between 1 and 2% for the rotational parameters and between 1 and 3% for the translational parameters.

In the course of refinement, the residual showed dramatic improvement, decreasing from $R = 42{\cdot}2$ to 40·7%, when the initial list of atomic coordinates was modified to reflect the amino acid sequence differences (~20 in the α and ~34 in the β chain) (Wong, 1975) between the horse and the deer hemoglobins by deleting all atoms not common to both molecules. The residual value increased steadily from 40·3% at 5·5 Å to a value of 43·0% as higher-resolution data were added (to 3·5 Å), signifying the differences of the structural details of the horse oxy and Hb(DIII) molecules.

The overall thermal parameter (B) and scale factor (K) were refined by selecting a 'high' (3·5 to 4·0 Å) and a 'low' (5·5 to 11·0 Å) order shell of data and requiring that the value for the overall thermal parameter be such that the overall scale factor which gave the minimum residual in both shells of data be the same.

The final R of 43·0% at 3·5 Å compares favorably to other macromolecular structures at similar resolution regardless of whether MIR or molecular replacement methods were used as the solution technique (Wishner, 1974; Ward *et al.*, 1975; Joynson *et al.*, 1970; Moews & Kretsinger, 1975; Fermi, 1975).

Description and discussion

From only unit-cell dimensions, space-group symmetry and the known shape of the hemoglobin molecule [a prolate spheroid with principal molecular axes X, Y and Z of 64, 50 and 55 Å, respectively, whose center is defined as the intersection of these axes (Perutz, Rossmann, Cullis, Muirhead, Will & North, 1960), a crude molecular packing model was postulated for the structure of sickling oxy-Hb(DIII) (Amma *et al.*, 1974). The postulated structure was that of an open honeycomb, essentially Fig. 6. Oriented single crystals in a Spurr matrix gave transmission electron micrographs of the *ab* and *ac* planes, Figs. 1 and 2 respectively, which clearly confirmed the postulated hexagonal nature of the packing and the existence of solvent channels.

However, neither the crude packing model nor the electron micrographs provide the precise angular and translational relations between molecules which are obtained from X-ray diffraction studies. Our low-resolution X-ray analysis is presented in terms of spherical molecules (Figs. 6 and 7) even though it is

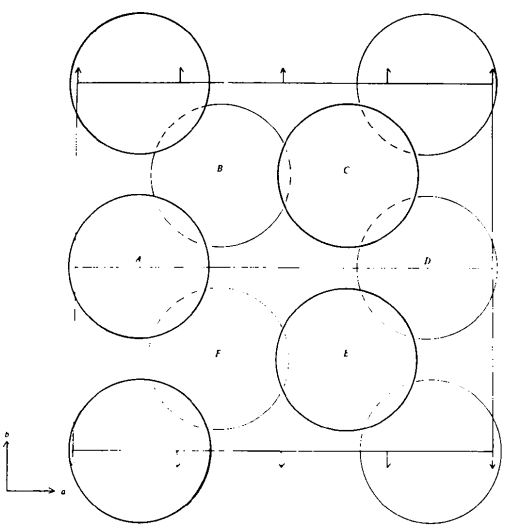

Fig. 6. A scaled representation ($a = 163$ Å) of the packing of spherical (55 Å diameter) Hb molecules as viewed down the [001] direction for one cell translation in the **a** direction and two in the **b** direction. The letters designating molecules are consistent with Fig. 7 to facilitate cross referencing. The pseudo-hexagonal array is represented by molecules (A, B, C, D, E, F) which clearly enclose the solvent channel.

Table 1. *A summary of the progress of the refinement associated with fitting horse oxyhemoglobin atomic coordinates to Hb(DIII) X-ray data of varying resolution*

The Eulerian rotational angles (θ_1, θ_2, θ_3), translational parameters (t_x, t_z), overall temperature (B) and scale (K) factors were independently varied (those parameters varied are designated ×) in a cyclic manner until the conventional residual, R, was minimized. The initial temperature factor of 30 Å^2 was improved (17 Å^2) by independent refinements of 'high' (3·5–4·0 Å) and 'low' (5·5–11·0 Å) order data shells. The initial list of atomic coordinates was modified (last column) to reflect the amino acid sequence differences between the horse and deer hemoglobins by deleting all atoms not common to both structures.

Residual	Data range	t_x	t_z	θ_1	θ_2	θ_3	K	B	Hb sequence
0·556*	11·0–5·5								Horse
0·538*	11·0–5·5	×	×						Horse
(0·425 for three-dimensional data)									
0·422	11·0–5·5	×	×	×	×	×			Horse
0·403	11·0–5·5	×	×	×	×	×			Deer†
0·476	11·0–3·5	×	×	×	×	×			Deer†
0·430	11·0–3·5						×	×	Deer†

* *h0l* data only.

† All atoms not common to horse and deer hemoglobins were deleted.

clear that many structural details are suppressed by this approach.

The X-ray results reveal a markedly distorted honeycomb which may be broken into either its component layers or its component strands to illustrate the nature of the distortions. One may visualize the structure as a series of layers of hexagonal arrays related by a simple translation in the **c** direction (~84° from the plane of the hexagonal array). The hexagonal repeat unit (*A, B, C, D, E, F* in Fig. 6) of the array has approximately $\bar{6}$ symmetry with adjacent molecules displaced ~26 Å along **c**. The idealized $\bar{6}$ symmetry is removed by a 13 Å displacement of molecule *A* and of molecule *D* in opposite directions along **a**. Since propagation of a single hexamer in the **c** direction causes the formation of a hollow fiber from six parallel filaments or fibrils (linear arrays of molecules), the honeycomb network can be constructed from interconnected hollow fibers parallel to **c**.

Alternatively one may visualize the structure as arising from an aggregation of antiparallel strands or fibrils (see definition above). The observed structural distortion can be introduced by moving adjacent fibrils 26 Å out of register in **c**, tilting them 5° to **c*** and contracting the lattice dimension in the **b** direction by ~12% (**a** expands by 12%).

The important facet of this structure is that the pseudo-hexagonal unit and its **c** repeat mentioned above appears without any *a priori* assumptions or dependence upon models and is similar in size (170 × 140 Å with a 66 Å axial repeat) and geometry to the cell-free fibers of HbS found by electron microscopy (Finch *et al.*, 1973; Edelstein, Telford & Crepeau, 1973), ~180 × 180 × 64 Å. This hexagonal hollow fiber model is also supported by the recent results of Zwick (1975).

While the nature of the interfiber interaction in the red blood cell is the subject of some debate (White, 1974; Stetson, 1966; Murayama, 1966), it is clear that parallel bundles of fibers are observed by EM in both Hb(DIII) (Simpson & Taylor, 1974) and in HbS, especially in the spicules [protuberances which distort the erythrocytes in advanced sickling stages (White, 1974)]. This kind of aggregation is consistent with the series of interconnected fibers found in the X-ray structure of Hb(DIII). Therefore, our structure not only accounts directly for the features of the isolated fibers, but also for the further aggregation that occurs in the cells of Hb(DIII) and HbS.

Intermolecular distance calculations using model Hb(DIII) atomic coordinates clearly show that the contact region across the crystallographic twofold axis is uniquely β–β whereas in all other directions it is composed of combinations of α–β, α–α, and β–β contacts. We shall describe in detail the specific contact regions and residues involved after refinement of individual atomic positions.

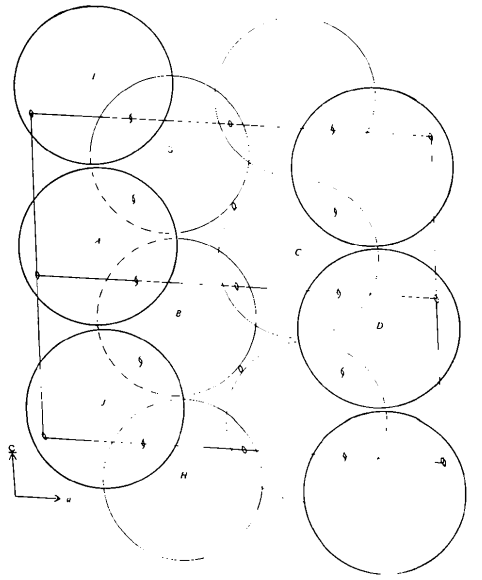

Fig. 7. A scaled representation ($a = 163$ Å) of the packing of spherical molecules (64 Å) viewed down **b**. This molecular size is slightly different from that of Fig. 4 to clarify the fibril interaction. Four of the six fibrils extending in the **c** direction are in this view. Two of these are composed of molecules *J, A, I* and *H, B, G* respectively.

We wish to thank Drs W. E. Love, E. E. Lattman, K. B. Ward and B. C. Wishner for their advice and encouragement during the course of this work, and acknowledge assistance from the staff of the Electron Microscopy Laboratory at the University of South Carolina.

This work was supported by the National Institutes of Health through grant No. HL-15158, and by the American and South Carolina Heart Associations, which provided financial support for GDS.

References

AMMA, E. L., SPROUL, G. D., WONG, S. & HUISMAN, T. H. J. (1974). *Ann. NY Acad. Sci.* **241**, 605–613.

BARNHART, M. I., HENRY, R. L. & LUSHER, J. M. (1974). *Sickle Cell*, edited by H. L. GROSS, SCOPE. Kalamazoo: Upjohn.

BERTLES, J. F. (1974). *Arch. Intern. Med.* **133**, 538–543.

CROWTHER, R. A. & BLOW, D. M. (1967). *Acta Cryst.* **23**, 544–548.

EDELSTEIN, S. J., TELFORD, J. N. & CREPEAU, R. H. (1973). *Proc. Natl. Acad. Sci. US*, **70**, 1104–1107.

FEHLHAMMER, H., SCHIFFER, M., EPP, O., COLMAN, P. M., LATTMAN, E. E., SCHWAGER, P., STEIGEMANN, W. & SCHRAMM, H. J. (1975). *Biophys. Struct. Mech.* **1**, 139–146.

FERMI, G. (1975). *J. Mol. Biol.* **97**, 237–256.

FINCH, J. T., PERUTZ, M. F., BERTLES, J. F. & DÖBLER, J. (1973). *Proc. Natl. Acad. Sci. US*, **70**, 718–722.

GASH, A. G., REEVES, E. H. & AMMA, E. L. (1976). Amer. Cryst. Assoc. Winter Meeting, Clemson Univ. Abstract SC6.

GIRLING, R. L., ABOLA, E. & WOOD, M. (1977). *J. Appl. Cryst.* **10**. To be published.

GIRLING, R. L., HOUSTON, T., SPROUL, G. D., SCHMIDT, W. C. JR, PLESE, C. & AMMA, E. L. (1976). Amer. Cryst. Assoc. Winter Meeting, Clemson Univ. Abstract B10.

HARRIS, M. J., WILSON, J. B. & HUISMAN, T. H. J. (1972). *Arch. Biochem. Biophys.* **151**, 540–548.

HUISMAN, T. H. J. (1972). *Advanc. Clin. Chem.* **15**, 149–253.

JOYNSON, M. A., NORTH, A. C. T., SARMA, V. R., DICKERSON, R. E. & STEINRAUF, L. K. (1970). *J. Mol. Biol.* **50**, 137–142.

KITCHEN, H., PUTNAM, F. W. & TAYLOR, W. J. (1964). *Science*, **144**, 1237–1239.

KITCHEN, H., PUTNAM, F. W. & TAYLOR, W. J. (1967). *Blood*, **29**, 867–877.

KOETZLE, T. F. (1974). Protein Data Bank, Brookhaven National Laboratory, Upton, NY.

LATTMAN, E. E. (1972). *Acta Cryst.* B**28**, 1065–1068.

LATTMAN, E. E. & LOVE, W. E. (1970). *Acta Cryst.* B**26**, 1854–1857.

LATTMAN, E. E., NOCKOLDS, C. E., KRETSINGER, R. H. & LOVE, W. E. (1971). *J. Mol. Biol.* **60**, 271–277.

MARKHAM, R., FREY, S. & HILLS, G. J. (1963). *Virology*, **20**, 88–102.

MARKHAM, R., HITCHBORN, J. H., HILLS, G. J. & FREY, S. (1964). *Virology*, **22**, 342–359.

MILNER, P. F. (1974). *Clin. Haematol.* **3**, 289–331.

MOEWS, P. C. & KRETSINGER, R. H. (1975). *J. Mol. Biol.* **91**, 201–228.

MURAYAMA, M. (1966). *Science*, **153**, 145–149.

NORTH, A. C. T., PHILLIPS, D. C. & MATHEWS, F. S. (1968). *Acta Cryst.* A**24**, 351–359.

PERUTZ, M. F., MUIRHEAD, H., COX, J. M. & GOAMAN, L. C. G. (1968). *Nature, Lond.* **219**, 131–139.

PERUTZ, M. F., ROSSMANN, M. G., CULLIS, A. F., MUIRHEAD, H., WILL, G. & NORTH, A. C. T. (1960). *Nature, Lond.* **185**, 416–422.

PROTHERO, J. W. & ROSSMANN, M. G. (1964). *Acta Cryst.* **17**, 768–769.

ROSSMANN, M. G. (1972). *The Molecular Replacement Method.* New York: Gordon and Breach.

ROSSMANN, M. G. & BLOW, D. M. (1962). *Acta Cryst.* **15**, 24–31.

SCHMID, M. F., HERRIOTT, J. R. & LATTMAN, E. E. (1974). *J. Mol. Biol.* **84**, 97–101.

SCHMIDT, W. C. JR, GIRLING, R. L., SPROUL, G. D. & AMMA, E. L. (1976). Amer. Cryst. Assoc. Winter Meeting, Clemson Univ. Abstract B9.

SIMPSON, C. F. & TAYLOR, W. J. (1974). *Blood*, **43**, 899–906.

SPURR, A. R. (1969). *J. Ultrastruct. Res.* **26**, 31–43.

STETSON, C. A. (1966). *J. Exp. Med.* **123**, 341–346.

STEWART, J. M., KRUGER, G. J., AMMON, H. L., DICKINSON, C. & HALL, S. R. (1972). The X-RAY system – version of June 1972. Tech. Rep. TR-192, Computer Science Center, Univ. of Maryland, College Park, Maryland.

STOUT, G. H. & JENSEN, L. H. (1968). *X-ray Structure Determination: A Practical Guide*, p. 457. London: Macmillan.

TAYLOR, W. J. & EASLEY, C. W. (1974). *Ann. NY Acad. Sci.* **241**, 594–604.

TOLLIN, P. (1969). *J. Mol. Biol.* **45**, 481–490.

WARD, K. B., WISHNER, B. C., LATTMAN, E. E. & LOVE, W. E. (1975). *J. Mol. Biol.* **98**, 161–177.

WATSON, M. L. (1958). *J. Biophys. Biochem. Cytol.* **4**, 475–478.

WHITE, J. G. (1974). *Arch. Intern. Med.* **133**, 545–562.

WISHNER, B. C. (1974). Ph.D. Thesis, The Johns Hopkins University.

WONG, S. C. (1975). Ph.D. Thesis, Medical College of Georgia.

ZEPPEZAUER, M. (1971). *Methods Enzymol.* **22**, 253–266.

ZWICK, M. (1975). Third East Coast Protein Crystallography Workshop, Lenox, Mass. Paper MS9.